IET Control Theory & Applications

Research Article

IET Journals
The Institution of Engineering and Technology

Flocking motion of multi-agent system by dynamic pinning control

ISSN 1751-8644
Received on 8th September 2016
Revised 21st November 2016
Accepted on 25th December 2016
E-First on 24th January 2017
doi: 10.1049/iet-cta.2016.1150
www.ietdl.org

Jingying Gao[1], Xu Xu[1] ✉, Nan Ding[1], Eric Li[2]

[1]*College of Mathematics, Jilin University, 2699 Qianjin Street, Changchun, 130012, People's Republic of China*
[2]*Department of Mechanical and Automation Engineering, The Chinese University of Hong Kong, Shatin, NT, Hong Kong, People's Republic of China*
✉ *E-mail: xuxu@jlu.edu.cn*

Abstract: The flocking motion in multi-agent system with switching topology is investigated in this study. A dynamic pinning control algorithm (DPCA) is developed to generate a stable flocking motion for all the agents without the assumption of connectivity or initial connectivity of the network. For the switching network, the network topology may be varied with time. All the agents at each topology switching time are regrouped into some connected subgroups, and the agent with the highest degree in each subgroup is selected as the informed agents. Based on LaSalle Invariance Principle, it is proved that the proposed DPCA ensures that the velocities of all the agents approach to that of the virtual leader asymptotically, no collision happens between the agents, and the system approaches to a configuration that minimises the global potentials. Moreover, the convergent rate and the computational cost of the proposed algorithm are investigated. The proposed DPCA is also applied to the situation where the virtual leader travels with a varying velocity. Numerical simulations demonstrate the stability and efficiency of the proposed algorithm.

1 Introduction

In the recent decades, flocking problems of multiple agents have attracted a great attention in many disciplines including animal behaviour, physics & biophysics, social science, and computer science. Researchers have put a lot of efforts to understand how a group of birds, school of fish, crowds of people, or man-made mobile autonomous agents can cooperate together without centralised control [1, 2].

Flocking is the phenomenon that a large number of agents use the limited environmental information and simple rules to organise into a coordinated motion. The classical flocking model proposed by Reynolds [3] consists of three heuristic rules: (i) separation: steer to avoid collision with nearby flock-mates; (ii) alignment: attempt to match velocity with nearby flock-mates; and (iii) cohesion: attempt to stay close to nearby flockmates. Over the last few years, many improvements of these three rules and additional rules have been suggested, such as rendezvous [4], consensus [5, 6], alignment [7, 8], and formation control [9]. Furthermore, there are various analytical tools such as Lyapunov-based approach [10, 11], graph theories [12, 13], infinite matrix products [14], and the artificial potentials [15] for modelling and analysing the flocking and the related cooperative behaviours.

The most of flocking results critically rely on an assumption of connectivity of the underlying network [16–25]. However, due to the switching property of the multi-agent network, it is not easy or rather impractical to keep network connectivity at all time. For example, in the unmanned aerial vehicles (UAVs) formation flight, it maybe encounter some static or dynamic obstacles. Sometimes the UAV agents have to be disconnected each other to avoid or bypass these obstacles. It is of practical significance to consider the switching topology.

On the other hand, it might be impossible or unnecessary to establish a direct control of each node for the large scale network. Pinning control is a very effective method by adding a control input to a fraction of nodes in the network [26, 27]. Luo *et al.* [28] studied the problem of flocking control combined with topology optimisation strategy for multi-agent systems. Su *et al.* [29] investigated the flocking control of multi-agent system via pinning control strategy. However, in his work, the network cannot maintain the connectivity; the algorithm does not achieve the three basic rules of Reynolds. In this paper, a simple dynamic pinning control algorithm (DPCA) is proposed to guarantee the flocking motion for all the agents. The main contributions of this paper are as follows: (i) without any assumption of connectivity or initial connectivity of the network; (ii) the network is regrouped sometimes to generate the connected subgroups; (iii) the agent with the highest degree in each subgroup is selected as the informed agent; and (iv) the effects of the navigational feedback coefficients on the convergence of the algorithm are discussed.

The remaining of this paper is organised as follows: Section 2 gives the introduction of the flocking problem. Sections 3 and 4 present the details on the DPCS and the main features of the proposed algorithm. Numerical experiments are shown in Section 5 to verify the theoretical analysis. Finally, Section 6 concludes this work.

2 Preliminaries

Consider n agents moving in a m-dimensional Euclidean space. The motion of each agent is described by

$$\begin{cases} \dot{q}_i = p_i \\ \dot{p}_i = u_i, \quad i = 1, 2, \ldots, n \end{cases} \tag{1}$$

where $q_i \in \mathbf{R}^m$ and $p_i \in \mathbf{R}^m$ are the position and velocity vectors of agent i, respectively; $u_i \in \mathbf{R}^m$ is the control input acting on the agent i, which consists of three components

$$u_i = f_i^{\alpha} + f_i^{\beta} + f_i^{\gamma}, \tag{2}$$

where f_i^{α} aims at coping with separation and cohesion with local attractive or repulsive potential; f_i^{β} regulates the velocity of agent to the weighted average velocity of its flockmates; and f_i^{γ} is a navigational feedback term to drive the agents to track the virtual leader described by

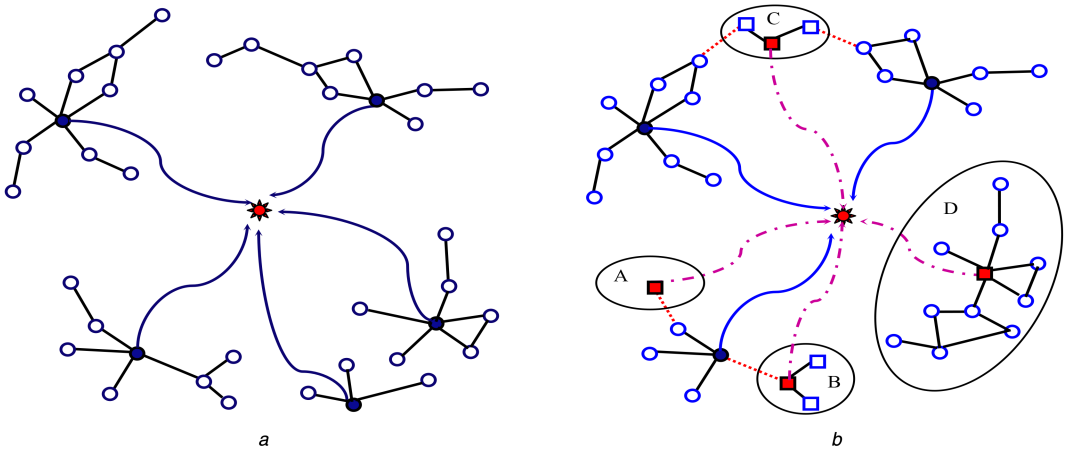

Fig. 1 *Illustration of dynamic pinning control algorithm*

(a) Network topology before regrouping, ***(b)*** Network topology after regrouping. Solid straight lines represent the real links between two agents; dashed straight lines in *(b)* are the disconnected link; solid curves are the connection between informed agents and the virtual leader; dot dashed curves in Fig. 1*b* are new added connection between the informed agents and the virtual leader after regrouping; in Fig. 1*b*, subgroup A only has a separated agent disconnecting from a subgroup; subgroup B consists of some agents disconnecting from a subgroup. In subgroup C, some type II uninformed agents disconnecting from the different subgroups form a new subgroup by re-accessing links between the agents. In subgroup D, two disconnected subgroups form a connected subgroup by re-accessing links

$$\begin{cases} \dot{q}_0 = p_0 \\ \dot{p}_0 = f_0(q_0, p_0) \end{cases} \tag{3}$$

where $q_0, p_0 \in \mathbf{R}^m$ are the position and velocity vectors of the virtual leader, respectively; and $f_0(q_0, p_0)$ is the control input of the virtual leader.

The virtual leader is used to provide the reference path for the agents to reach the predefined destination. For example, in the UAVs formation flight, the virtual leader looks like a preplanned sailing route or a manual instruction coming from the commander on the ground. The agents in the UAV group may encounter complex situations such as avoiding obstacles. They usually do not strictly follow the predefined sailing route or the command at every moment. However, the predefined path or the command will be referenced to planning their flight path. In this work, the switching topological structure is considered. Each agent has a limited communication capability, and the neighbouring set of the ith agent at time t is denoted as

$$N_i(t) = \{j \in V | \parallel q_i(t) - q_j(t) \parallel < r, j \neq i\}, \tag{4}$$

where $\parallel \cdot \parallel$ is the Euclidean norm, and r is the sensing radius. The neighbouring set $N_i(t)$ of ith agent changes dynamically as a function of distance between the agents as follows:

i. The initial links are generated by

$$E(0) = \{(i, j) | 0 < \parallel q_i(0) - q_j(0) \parallel < r, \ i, j \in V\};$$

ii. If $(i, j) \notin E(t_-)$ and $\parallel q_i(t) - q_j(t) \parallel < r$, then (i, j) is a new link to be added to $E(t)$;

iii. If $(i, j) \in E(t_-)$ and $\parallel q_i(t) - q_j(t) \parallel \geq r$, then the link (i, j) is deleted from $E(t)$.

3 Dynamic pinning control algorithm

3.1 Details on the DPCA

In the DPCA, the initial network $G(t_0)$ is first divided into $l(t_0)$ connected subnetworks $G_1, G_2, \ldots, G_{l(t_0)}$ as shown in Fig. 1*a*. These subnetworks satisfy that $G(t_0) = G_1 \cup G_2 \cup \cdots \cup G_{l(t_0)}$, and $G_i \cap G_j = \phi$ for $i \neq j$. In this paper, only one agent with the highest degree in each connected subnetwork is selected as the informed agent (solid circles in Fig. 1*a*). The informed agent can 'receive' the feedback information from the virtual leader directly. The others are called as the uninformed agents (hollow nodes in Fig. 1). The uninformed agents are divided into two types: type I and type II uninformed agents. An agent is called type I uninformed agent if there is a path between this agent and any one of the informed agents; otherwise, it is called type II uninformed agent [29].

For the switching topology, the edges between any two agents may be disconnected sometimes, and thus generates the type II uninformed agents. To track the virtual leader, all the agents are regrouped into some new connected subgroups at switching time using the algorithm depth first search (DFS) or breadth first search (BFS) [30]. The topology switching time is the moment that the changing of the neighbouring set of an agent, which include that (i) generates type II uninformed agents; (ii) some disconnected subgroups form a new connected subgroup; and (iii) the topology of one connected subgroup has changed. After regrouping, the neighbouring set of each agent is invariable before the next switching time. Then, one agent with the highest degree in each connected subgroup is selected as the informed agent. Moreover, the virtual links are added between each informed agent (solid and dash curve lines in Fig. 1*b*) and the virtual leader for an informed agent to receive the information of the leader. Therefore, there are no type II uninformed agents after regrouping.

The control input for the agent i is given as

$$\begin{aligned} u_i(t) = &- \sum_{j \in N_i(t)} \nabla_{q_i} \psi_\alpha(\parallel q_j - q_i \parallel_\sigma) \\ &+ \sum_{j \in N_i(t)} a_{ij}(t)(p_j - p_i) + h_i(t)[c_1(q_0 - q_i) + c_2(p_0 - p_i)] \\ &i = 1, 2, \ldots, n \end{aligned} \tag{5}$$

where $c_1, c_2 > 0$, $h_i(t) = 1$ for the informed agent i, $h_i(t) = 0$ for the uninformed agent i. The potential function $\psi_\alpha(z)$ and the adjacent matrix $A(t) = \{a_{ij}(t)\}_{n \times n}$ are denoted as those in [18]. Function $\psi_\alpha(z)$ in (5) is a smooth pairwise attractive/repulsive potential [defined in (6)] with a finite cut-off at $r_\alpha = \parallel r \parallel_\sigma$ and a global minimum at $z = d_\alpha \equiv \parallel q_j - q_i \parallel_\sigma, \forall j \in N_i(q)$,

$$\psi_\alpha(z) = \int_{d_\alpha}^{z} \phi_\alpha(s)\, \mathrm{d}s, \tag{6}$$

with

$$\begin{cases} \phi_\alpha(z) = \rho_h(z/r_\sigma)\phi(z - d_\alpha) \\ \phi(z) = \frac{1}{2}[(a+b)\sigma_1(z+c) + (a-b)], \\ \sigma_1(z) = z/\sqrt{1+z^2} \end{cases} \tag{7}$$

where $\phi(z)$ is an uneven sigmoidal function which parameters satisfy that $0 < a \leq b$, $c = |a-b|/\sqrt{4ab}$ to guarantee $\phi(0) = 0$.

The σ-norm of a vector is defined as $\| z \|_\sigma = (1/\varepsilon)[\sqrt{1 + \| z \|^2} - 1]$ with a parameter $\varepsilon > 0$. A bump function is a scalar function $\rho_h(z)$ that smoothly varies between 0 and 1. One possible choice is the following bump function:

$$\rho_h(z) = \begin{cases} 1 & z \in [0, h) \\ \frac{1}{2}\left[1 + \cos\left(\pi \frac{z-h}{1-h}\right)\right] & z \in [h, 1], \\ 0 & \text{otherwise} \end{cases}$$

where $h \in (0, 1)$. The details of function $\psi_\alpha(z)$ can be seen in [18].

The control process is described as following the *flocking algorithm I:*

Step 1: Set all the parameters and initialise position $q_i(0)$ and velocity $p_i(0)$ of all the agents ($i = 0, 1, 2, \ldots, n$). Set time $t = 0$.

Step 2: Regrouping all the agents as $l(t)$ subgroups at the topology switching time using the algorithm DFS (or BFS).

Step 3: Take the highest degree agent in each subgroups as an informed agent.

Step 4: Add a virtual link from each informed agent to the virtual leader.

Step 5: Update the positions and velocities of all the agents using (5) for time interval Δt.

Step 6: The process is ended for two cases (the velocities of all the agents reach consensus, or the maximum number of iteration is achieved); otherwise set $t = t + \Delta t$, go to step 7.

Step 7: Search the entire network: (i) if there exist the type II uninformed agents at time t, or some disconnected components shown at $t - \Delta t$ form a new subgroup at time t, go to step 2; (ii) if the two cases mentioned above do not appear, but the topology of some subgroups has changed, go to step 3; (iii) if the topology of the entire network does not change compared with that at time $t - \Delta t$, go to step 5.

Remark 1: The reason that the agent with the highest degree is selected as the informed agent is that the degree of node is the simplest way to measure the influence and importance of a node. This is one key difference between the proposed algorithm and that in [29].

Remark 2: After regrouping, all the generated subgroups are connected between two adjacent switching time. This gives a simple way to generate the connected subnetworks.

Remark 3: The network topological is invariable between two adjacent switching time slots.

Remark 4: The informed agents in the proposed algorithm often change; whereas the informed agents do not change in [29].

3.2 Stability analysis of the algorithm

Define the system energy

$$Q(t) = \frac{1}{2}\sum_{i=1}^{n}[U_i + (p_i - p_0)^{\mathrm{T}}(p_i - p_0)], \tag{8}$$

where

$$U_i = \sum_{j=1, j\neq i}^{n} \psi_\alpha(\| q_{ij} \|_\sigma) + h_i(t)c_1(q_i - q_0)^{\mathrm{T}}(q_i - q_0). \tag{9}$$

The matrix analysis and algebraic graph theory [31, 32] are employed for discussions.

Theorem 1: Consider a system of n mobile agents, each with (1), steered by the control protocol (5) and the algorithm I. Suppose that the initial energy $Q(t_0)$ is finite. Then

i. The velocities of all the agents approach to the velocity of the virtual leader asymptotically. Average position of informed agents asymptotically approaches the position of the virtual leader.
ii. The system approaches to a configuration that minimises the potentials of all the agents.
iii. No collision happens between the mobile agents.

Proof:

(1) Let $t_1, t_2, \ldots$ denote a series of switching time so that the switching topology $G(t)$ is the same within each of the intervals $[t_y, t_{y+1})$ for $y = 0, 1, \ldots$. Due to the switching topology, the total energy function $Q(t)$ is discontinuous at each switching time, but differential in each interval $[t_y, t_{y+1})$. Let $\tilde{q}_i = q_i - q_0$, $\tilde{p}_i = p_i - p_0$, $q_{ij} = q_i - q_j$ and $\tilde{q}_{ij} = \tilde{q}_i - \tilde{q}_j$. Hence the control protocol (5) for agent i is rewritten as

$$\begin{aligned} u_i = &- \sum_{j\in N_i(t)} \nabla_{\tilde{q}_i}\psi_\alpha(\| \tilde{q}_{ij} \|_\sigma) \\ &- \sum_{j\in N_i(t)} a_{ij}(q)(\tilde{p}_i - \tilde{p}_j) - h_i(t)[c_1\tilde{q}_i + c_2\tilde{p}_i], \end{aligned} \tag{10}$$

and the non-negative energy function (8) can be written as

$$Q(t) = \frac{1}{2}\sum_{i=1}^{n}(U_i + \tilde{p}_i^{\mathrm{T}}\tilde{p}_i), \tag{11}$$

where

$$U_i(\tilde{q}) = \sum_{j=1, j\neq i}^{n} \psi_\alpha(\| \tilde{q}_{ij} \|_\sigma) + h_i(t)c_1\tilde{q}_i^{\mathrm{T}}\tilde{q}_i. \tag{12}$$

Clearly, $Q(t)$ is a positive semi-definite function, where $\tilde{p} = \mathrm{col}(\tilde{p}_1, \tilde{p}_2, \ldots, \tilde{p}_n) \in \mathbf{R}^{mn}$ and $\tilde{q} = \mathrm{col}(\tilde{q}_1, \tilde{q}_2, \ldots, \tilde{q}_n) \in \mathbf{R}^{mn}$. Due to the symmetry of the pairwise potential function and the adjacent matrix, we have

$$\nabla_{\tilde{q}_{ij}}\psi_\alpha(\| \tilde{q}_{ij} \|_\sigma) = \nabla_{\tilde{q}_i}\psi_\alpha(\| \tilde{q}_{ij} \|_\sigma) = -\nabla_{\tilde{q}_j}\psi_\alpha(\| \tilde{q}_{ij} \|_\sigma). \tag{13}$$

The time derivative of $Q(t)$ along the trajectories of the agents and the virtual leader is given by

$$\begin{aligned} \dot{Q}(t) &= \sum_{i=1}^{n}\sum_{j\in N_i(t)} \tilde{p}_i^{\mathrm{T}}\nabla_{\tilde{q}_i}\psi_\alpha(\| \tilde{q}_{ij} \|_\sigma) \\ &\quad + \sum_{i=1}^{n} h_i(t)c_1\tilde{p}_i^{\mathrm{T}}\tilde{q}_i + \sum_{i=1}^{n}\tilde{p}_i^{\mathrm{T}}u_i \\ &= -\tilde{p}^{\mathrm{T}}[(L(t) + c_2H(t)) \otimes I_m]\tilde{p} \leq 0 \end{aligned} \tag{14}$$

where $H(t) = \mathrm{diag}[h_1(t), h_2(t), \ldots, h_n(t)]$.

In deriving (14), we have used that both $L(t)$ and $H(t)$, thus $L(t) + c_2H(t)$ are positive semi-definite matrices. The fact $\dot{Q}(t) \leq 0$ implies that $Q(t)$ is a non-increasing function when $t \in [t_y, t_{y+1})$, $y = 0, 1, 2, \ldots$.

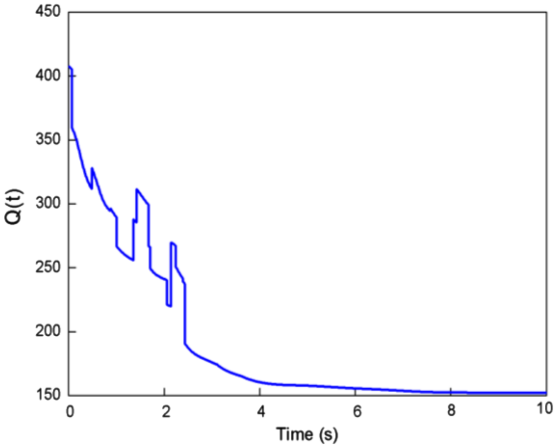

Fig. 2 *Illustration of total energy function with time*

Denote t_y^- and t_y as the switching time before and after regrouping. The total energy function $Q(t_y^-)$ may not be equal to $Q(t_y)$ at the switching times. The main reason for the discontinuity of the total energy is the emergence of the type II uninformed agents, which result in the increase of the total energy function (8) (see Fig. 2). However, at each interval $[t_y, t_{y+1})$ $(y = 0, 1, 2, \ldots)$, $Q(t)$ decreases with the increase of time, which implies that all the agents gradually adjust their position to the desired distance and their velocity to that of the virtual leader. It will reduce the emergence of type II agents and the difference of the energy function $\Delta Q = Q(t_y) - Q(t_y^-)$. After a finite time T_0, the size of the largest subgroup will increase and no more type II uninformed agents will emerge.

In the following analysis, we only consider the case when $t > T_0$. For any $c > 0$, let $\Omega = \{[\tilde{q}^{\mathrm{T}}, \tilde{p}^{\mathrm{T}}]^{\mathrm{T}} \in \mathbf{R}^{2mn} | Q(\tilde{q}, \tilde{p}) \le c\}$ denote the level sets of Q. Following from the aforementioned conclusions, Ω is an invariant set. It can be obtained from (11) that $\tilde{p}_i^{\mathrm{T}}\tilde{p}_i \le 2c,\ i = 1, 2, \ldots, n$. Hence, $\| \tilde{p}_i \|$ are bounded. It can be also deduced that $\| \tilde{q}_i \|$, $i = 1, 2, \ldots, n$ are bounded, no matter whether the agent is informed or is connected to the virtual leader indirectly. This shows that the set Ω is compact, and Ω is an invariant compact set. It follows from the LaSalle invariance principle [31] that all trajectories of the agents that start from set Ω will converge to the largest invariant set inside the region

$$S = \{[\tilde{q}^{\mathrm{T}}, \tilde{p}^{\mathrm{T}}]^{\mathrm{T}} \in \mathbf{R}^{2mn} | \dot{Q} = 0\}.$$

We have that both $L(t) \otimes I_m$ and $c_2 H(t) \otimes I_m$ are positive semi-definite. Thus, it follows from (14) that $\dot{Q}(t) = 0$ if and only if $-\tilde{p}^{\mathrm{T}}(L(t) \otimes I_m)\tilde{p} = 0$ and $-\tilde{p}^{\mathrm{T}}(H(t) \otimes I_m)\tilde{p} = 0$.

We assume that network $G(t)$ has $l(t)$ connected subgroups, and there are $\rho_k(t), k = 1, 2, \ldots, l(t)$ agents within each subgroup. For any time $t \ge 0$, there exists an orthogonal permutation matrix $P(t) \in \mathbf{R}^{n \times n}$ such that $L(t)$ can be transformed into a block diagonal matrix of the form

$$\check{L}(t) = P(t)L(t)P(t)^{\mathrm{T}} = \mathrm{diag}(L_1(t), L_2(t), \ldots, L_{l(t)}(t)),$$

where $L_k(t) \in \mathbf{R}^{\rho_k(t) \times \rho_k(t)}, k = 1, 2, \ldots, l(t)$ is the Laplacian matrix associated with the kth connected component of the graph. The indices of the state vector can be rearranged such that

$$\check{\tilde{p}} = [\tilde{p}^{1\mathrm{T}}, \tilde{p}^{2\mathrm{T}}, \ldots, \tilde{p}^{l(t)\mathrm{T}}]^{\mathrm{T}} = (P(t) \otimes I_m)\tilde{p},$$

where $\tilde{p}^k = [\tilde{p}_1^k, \ldots, \tilde{p}_{\rho_k(t)}^k]^{\mathrm{T}}$ is the difference of the velocity vector of the $\rho_k(t)$ agents within the kth connected component. We then have

$$\begin{aligned}\check{\tilde{p}}^{\mathrm{T}}(\check{L}(t) \otimes I_m)\check{\tilde{p}} &= [(P(t) \otimes I_m)\tilde{p}]^{\mathrm{T}}(\check{L}(t) \otimes I_m)[(P(t) \otimes I_m)\tilde{p}] \\ &= \tilde{p}^{\mathrm{T}}(L(t) \otimes I_m)\tilde{p}.\end{aligned}$$

Therefore

$$-\tilde{p}^{\mathrm{T}}(L(t) \otimes I_m)\tilde{p} = -\check{\tilde{p}}^{\mathrm{T}}(\check{L}(t) \otimes I_m)\check{\tilde{p}} = -\sum_{k=1}^{l(t)} \tilde{p}^{k\mathrm{T}}(L_k(t) \otimes I_m)\tilde{p}^k.$$

Clearly, $-\tilde{p}^{\mathrm{T}}(L(t) \otimes I_m)\tilde{p} = 0$ if and only if $-\tilde{p}^{k\mathrm{T}}(L_k(t) \otimes I_m)\tilde{p}^k = 0, 1 \le k \le l(t)$. As the Laplacian matrix $-\tilde{p}^{k\mathrm{T}}(L_k(t) \otimes I_m)\tilde{p}^k = 0$ is equivalent to $\tilde{p}_1^k = \cdots = \tilde{p}_{\rho_k(t)}^k$ for $1 \le k \le l(t)$, the velocity errors of all the agents in the same connected component $G_k(t)$ are identical. Similarly, we have

$$-\tilde{p}^{\mathrm{T}}(H(t) \otimes I_m)\tilde{p} = -\sum_{k=1}^{l(t)} \tilde{p}^{k\mathrm{T}}(H_k(t) \otimes I_m)\tilde{p}^k,$$

where $H_k(t) \in \mathbf{R}^{\rho_k(t) \times \rho_k(t)}$ is the diagonal matrix associated with the kth connected component with the ith diagonal element which is equal to one for an informed agent and zero for an uninformed agent $(1 \le i \le \rho_k(t))$.

Clearly, $-\tilde{p}^{\mathrm{T}}(H(t) \otimes I_m)\tilde{p} = 0$ if and only if $-\tilde{p}^{k\mathrm{T}}(H_k(t) \otimes I_m)\tilde{p}^k = 0,\ 1 \le k \le l(t)$, which implies that the velocity errors between the informed agents and the virtual leader is zero.

In the proposed algorithm, only one node with the highest degree in each subgroup is selected as an informed agent. It is assumed that the first agent in each connected component is an informed agent, then we have $\tilde{p}_1^k = 0,\ 1 \le k \le l(t)$. According to the above results, we have $\tilde{p}_1^k = \cdots = \tilde{p}_{\rho_k(t)}^k = 0$, for $1 \le k \le l(t)$, which indicates that $p_1 = p_2 = \cdots = p_n = p_0$.

We know that all the agents track the virtual leader with the same velocity and maintain a constant relative distance with their neighbours asymptotically, i.e.

$$\dot{p}_1 = \dot{p}_2 = \cdots = \dot{p}_n = \dot{p}_0 = 0.$$

From (5), we have

$$u_i(t) = -\sum_{j \in N_i(t)} \nabla_{q_i} \psi_\alpha(\| q_{ij} \|_\sigma) - h_i(t)c_1(q_i - q_0).$$

Since

$$\sum_{i=1}^n u_i(t) = -\sum_{i=1}^n \sum_{j \in N_i(t)} \nabla_{q_i} \psi_\alpha(\| q_{ij} \|_\sigma) - \sum_{i=1}^n h_i(t)c_1(q_i - q_0) = 0,$$

we have

$$\sum_{i=1}^n h_i(t)(q_i - q_0) = l(t)\left(\frac{\sum_{i=1}^{l(t)} q_i}{l(t)} - q_0\right) = 0,$$

which indicates that the average position of informed agents asymptotically approaches the position of the virtual leader. This completes the proof of the part 1.

(2) Furthermore, the system trajectories converge to $S = \{[\tilde{q}^{\mathrm{T}}, \tilde{p}^{\mathrm{T}}]^{\mathrm{T}} \in \mathbf{R}^{2mn} | \dot{Q}(t) = 0\}$. In set S, velocity dynamics of agents become

$$u = \dot{\tilde{p}} = -[(\nabla_{q_1} U_1)^{\mathrm{T}}, (\nabla_{q_2} U_2)^{\mathrm{T}}, \ldots, (\nabla_{q_n} U_n)^{\mathrm{T}}]^{\mathrm{T}} = 0,$$

which indicates that the potential U_i, $i = 1, 2, \ldots, n$ of each agent is minimised when the velocities of all the agents converge to a common value. This completes the proof of the part 2.

(3) We first discuss the collision avoidance in time interval $t \in [t_0, t_1)$. Assume there exists a time $t_s \in [t_0, t_1)$ so that two distinct agents k and l collide, or $q_k(t_s) = q_l(t_s)$. Therefore, we have

$$\begin{aligned} V(q(t)) &= \frac{1}{2} \sum_i \sum_{j \neq i} \psi_\alpha(\| q_{ij} \|_\sigma) \\ &= \psi_\alpha(\| q_k - q_l \|_\sigma) + \frac{1}{2} \sum_{i \neq k, l} \sum_{j \neq i, k, l} \psi_\alpha(\| q_j - q_i \|_\sigma) \\ &\geq \psi_\alpha(\| q_k - q_l \|_\sigma) \end{aligned}$$

Hence, we have $V(q(t_s)) \geq \psi_\alpha(0)$. If we assume $Q(0) < \psi_\alpha(0)$, then from (14) we have $V(q(t)) \leq Q(t) \leq Q(0) < \psi_\alpha(0)$, for any $t \in [t_0, t_1)$, which is in contradiction with an earlier inequality $V(q(t_s)) \geq \psi_\alpha(0)$. Therefore, no two agents collide at any $t \in [t_0, t_1)$ if the assumption $Q(0) < \psi_\alpha(0)$ is satisfied.

On the other hand, if assumes $\psi_\alpha(0) \leq Q(t_0) < (\bar{k} + 1)\psi_\alpha(0)$ where $\bar{k} \in \mathbb{Z}_+$, then we have the result: no more than $\bar{k}$ distinct pairs of agents can possibly collide at sometimes. If the above conclusion As the discussions is incorrect, there must be at least $\bar{k} + 1$ distinct pairs of agents that collide at a given time $t_s \in [t_0, t_1)$. This implies that collective potential of the particle system at time t_s is at least $(\bar{k} + 1)\psi_\alpha(0)$. However, from $\dot{Q}(t) \leq 0$ we have $Q(0) \geq Q(t_s) = (\bar{k} + 1)\psi_\alpha(0)$. This contradicts the assumption that $Q(t_0) < (\bar{k} + 1)\psi_\alpha(0)$, hence, no more that no more than $\bar{k}$ distinct pairs of agents can possibly collide at sometimes. Finally, with $\bar{k} = 0$, i.e. $Q(0) < \psi_\alpha(0)$, no two agents ever collide at any time $t \in [t_0, t_1)$.

As the discussions in the proof of part 1, due to the changing of the neighbouring set of an agent at switching time t_y, the energy function $Q(t_y^-)$ at time t_y^- is not equal to $Q(t_y)$ generally. The main reason for this discontinuity is the emergence of type II uninformed agents. According to the discussion in [29], a very small proportions of type II uninformed agents will be generated in the network at time t_k^-. In addition, based on the proposed algorithm, the newly added virtual connections will decrease the energy function. Hence, the difference of the energy function $\Delta Q = Q(t_y) - Q(t_{y-1})$ is very small. So, if we choose $Q(0) < \psi_\alpha(0)$ (or choose a large enough $\psi_\alpha(0)$), then the assumption $Q(t_y) < \psi_\alpha(0)$ still holds at any topology switching time t_y. Accordingly, similar to the above discussion, we prove that no collision happens between the agents at any time interval $t \in [t_y, t_{y+1})$, $y = 0, 1, 2, \ldots$. This completes the proof of the part 3. □

4 Flocking for a virtual leader with a varying velocity

For the virtual leader with a varying velocity, the following control protocol is proposed:

$$\begin{aligned} u_i = &- \sum_{j \in N_i(t)} \nabla_{q_i} \psi_\alpha(\| q_j - q_i \|_\sigma) \\ &+ \sum_{j \in N_i(t)} a_{ij}(t)(p_j - p_i) \\ &+ h_i(t)[c_1(q_0 - q_i) + c_2(p_0 - p_i)] + f_0(q_0, p_0), \\ &i = 1, 2, \ldots, n \end{aligned} \tag{15}$$

where $f_0(q_0, p_0)$ is the acceleration input of the virtual leader and all other parameters are the same as those in (5). The flocking algorithm for the virtual leader with a varying velocity is similar as the algorithm I, except the algorithm updating the positions and velocities of the agents using (15) in step 5.

Theorem 2: Consider a system of n mobile agents, each with (1), steered by the control protocol (15) and the algorithm II. Suppose that the initial energy $Q(t_0)$ is finite. Then

i. The velocities of all the agents approach to the velocity of the virtual leader asymptotically. The average position of the informed agents asymptotically approaches the position of the virtual leader.
ii. The system approaches to a configuration that minimises the potentials of all the agents.
iii. No collision happens between the mobile agents.

Proof: See the Appendix. □

5 Simulations and discussions

Example 1: Flocking with a virtual leader of a constant velocity. In this example, the simulations are performed on $n = 30$ agents moving in a two-dimensional space. The initial positions and velocities of n agents are chosen randomly from $[0, 25] \times [0, 25]$ and $[-1, 1] \times [-1, 1]$, respectively. The sensing radius is $r = 4$, the desired distance $d = 3.3$, $c_1 = 1, c_2 = 3$, and the rest of the parameters are set as same as those in [18]. The initial position and velocity of the virtual leader are $q_0(0) = [12, 12]^{\mathrm{T}}$ and $p_0 = [0.5, 0.5]^{\mathrm{T}}$. The virtual leader is assumed to have a constant velocity.

Fig. 3 presents the evolution process of topology at some times. In the figure, the solid circle is the informed agent, and the star denotes the virtual leader. The arrows in Fig. 3*f* represent the velocities of the agents. Fig. 3*a* shows the initial state of all the agents which are highly disconnected. We use the subscript of the informed agent to denote a subgroup. It is easy to see that the subgroups 26 and 17 in Fig. 3*a* form a new connected subgroup 17 in Fig. 3*b*, and subgroups 11 and 15 in Fig. 3*a* form another a new subgroup 7 in Fig. 3*b*; subgroups 17 and 14 in Fig. 3*b* form a new connected subgroup 17 in Fig. 3*c*, and subgroup 7 and agent 30 (separated agent) in Fig. 3*b* form a new connected subgroup 7 in Fig. 3*c*. There are type II uninformed agents 8, 9, and other type II uninformed agent 21 in Fig. 3*d*, then we choose agents 9 and 21 as new informed agents. As time goes on, the size of the largest subgroup increases and the number of the connected subgroups decreases (see Figs. 3*b–e*). Eventually, all the agents are connected and have the same velocity with the virtual leader. The final distance between an agent and its neighbour is equal to d as shown in Fig. 3*f*.

Fig. 4*a* depicts the flocking trajectories of ten agents. It is clearly seen that all the agents regulate their positions to move ahead with steady state configurations eventually. Fig. 4*b* gives the number of the informed agents within 50 s. It is observed that the number of informed agents decreases with an increase of the time. However, sometimes, the number of the informed agents increases. This is because some new type II uninformed agents appear in the network, and we need to convert these new type II uninformed agents to type I uninformed agents which result in more informed agents. Figs. 4*c* and *d* show the difference of the position and

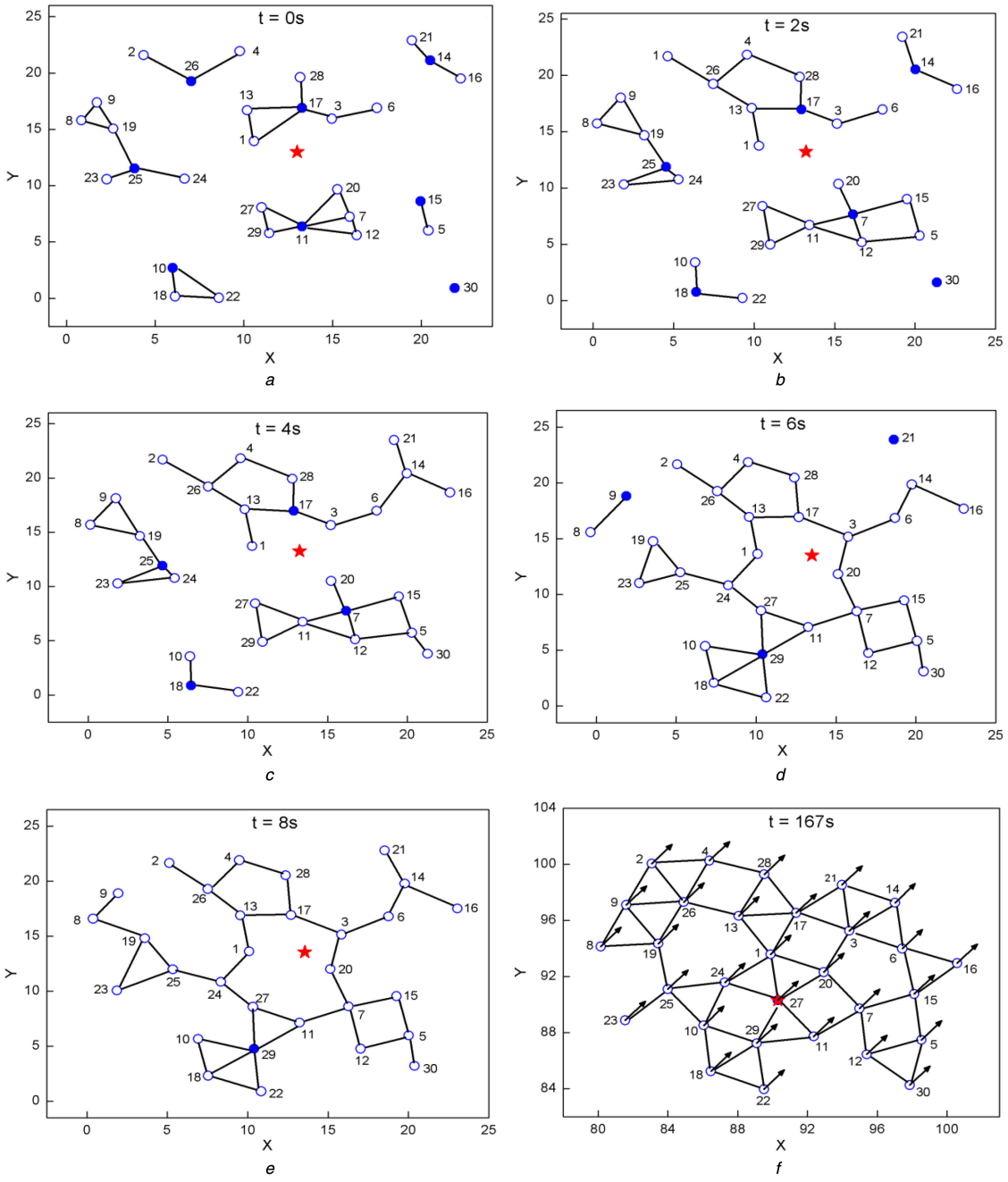

Fig. 3 *2D flocking for 30 agents applying the proposed flocking algorithm*
(a) Initial topology of 30 agents, ***(b)*** Network topology at 2 s, ***(c)*** Network topology at 4 s, ***(d)*** Network topology at 6 s, ***(e)*** Network topology at 8 s, ***(f)*** Final topology of 30 agents

velocity between the agents and the virtual leader defined as follows:

$$e_q = \frac{1}{l(t)}\sum_{i=1}^{l(t)} q_i - q_0, \quad e_p = \frac{1}{n}\sum_{i=1}^{n} p_i - p_0, \tag{16}$$

where $l(t)$ is the number of the informed agents. It is obviously shown from the figures that e_q and e_p gradually approach to zero, which indicates that the average positions of the informed agent and velocities of all the agents will converge to those of the virtual leader.

Example 2: Convergence and computational cost. In this example, a comparison is made for the convergent rate and the computational cost between the algorithm in [28] and the proposed algorithm in this work. The cost function is defined as follows:

$$\mathrm{Cf}(t) = \sum_{i=1}^{n} h_i(t)(c_1 + c_2) + \frac{1}{2}\sum_{i=1}^{n}\sum_{j \in N_i(t)} a_{ij}(t)\,. \tag{17}$$

The parameters in two algorithms are exactly the same as those in Example 1.

Fig. 5*a* gives a comparison of the total iterative number for achieving the flocking behaviour between two algorithms running ten times. It is found that the iterative number of the proposed algorithm (algorithm B) is always less than that of the algorithm in [28] (algorithm A). The average iterative number for the proposed algorithm is about 5600; while the algorithm A needs about 7000 iteration steps. It is also clearly shown from Fig. 5*b* that the computational cost of the proposed algorithm is also less than that of the algorithm A. These results indicate that the proposed algorithm has a better convergence rate and less computational cost than those of algorithm in [28].

Example 3: Discussions on the coefficients c_1, c_2. Fig. 6 shows the comparison for the convergent rate between the proposed algorithm

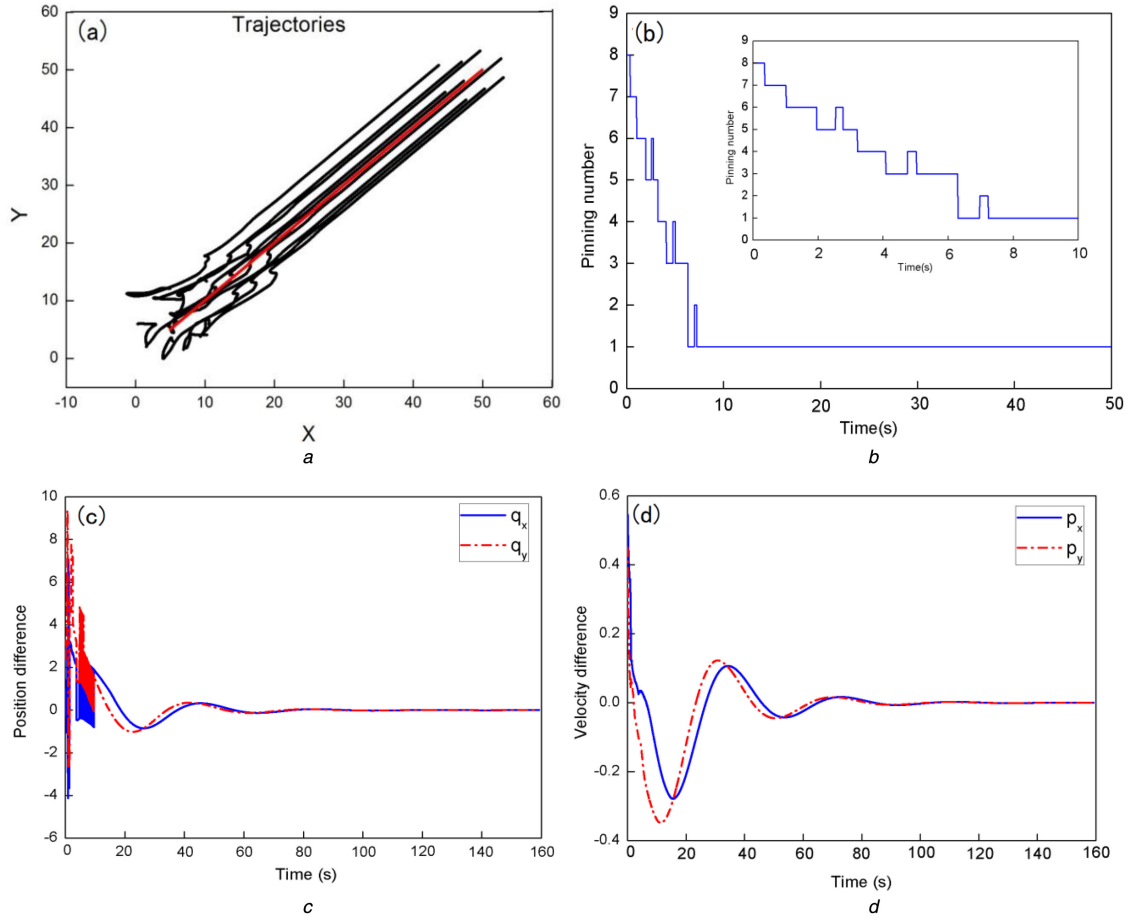

Fig. 4 *Simulation results of flocking for 30 agents*
(a) Trajectories of ten agents and the virtual leader, ***(b)*** Pinning number, ***(c)*** Position difference, ***(d)*** Velocity difference

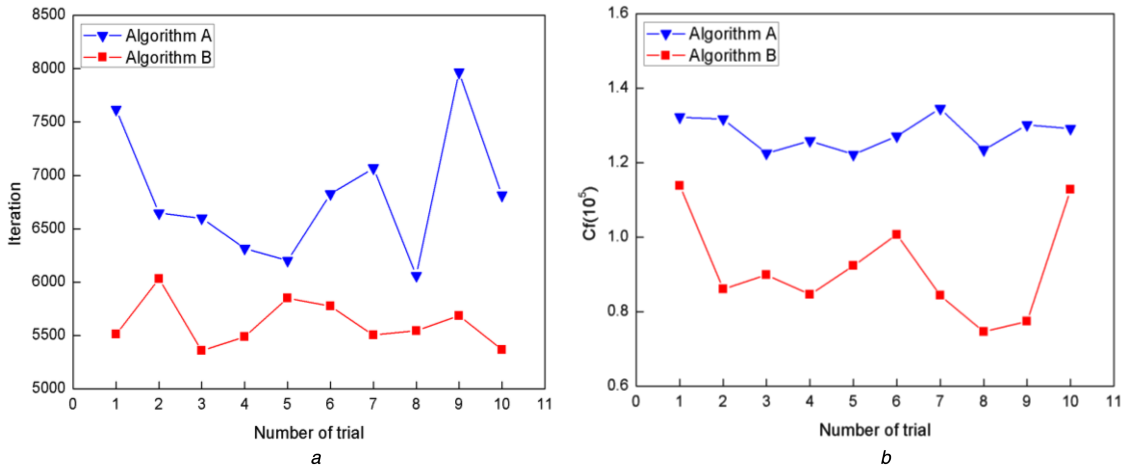

Fig. 5 *Comparisons of the convergence and the computational cost for two algorithms*
(a) Comparison of convergence of two algorithms, ***(b)*** Comparison of computational cost of two algorithms

pinning the highest degree node (algorithm B) and that pinning a randomly chosen one (algorithm A) in each subgroup. The parameters in this example are the same as those in Example 1.

Fig. 6*a* gives the comparison between two algorithms for fixed $c_2 = 3$, and c_1 is changed from 0.5 to 4.5; while Fig. 6*b* gives this comparison for fixed $c_1 = 1$, and c_2 is changed from 0.5 to 6. The result is the averaging values of over 30 realisations. It is clearly observed that the total iterative number of the proposed algorithm B is less than that of algorithm A, which means the proposed algorithm B takes less cost to achieve the flocking motion. With an increase of c_1 from 1 to 3.5 for fixed c_2, or c_2 from 3 to 6 for fixed c_1, the number of iterations is almost unchanged for the proposed algorithm, which indicates that the proposed algorithm is very robust regardless of the values of c_1 and c_2. This example has clearly validated that pinning the highest degree node in each subgroup is more stable and efficient than pinning randomly chosen one.

Example 4: Flocking with a virtual leader of varying velocity. In this example, the flocking motion of the agents following a virtual leader with a varying velocity is considered. The parameters in this simulation are the same as that in Example 1 except that the initial position and the velocity of the virtual leader are set as $q_0(0) = [10, 10]^{\mathrm{T}}$ and $p_0 = [2, 0]^{\mathrm{T}}$; the acceleration of the virtual leader is set as $f_0(q_0, p_0) = \cos(q_0)$.

Fig. 7*a* depicts the motion trajectories of three agents and the virtual leader with a varying velocity. Fig. 7*b* illustrates the number

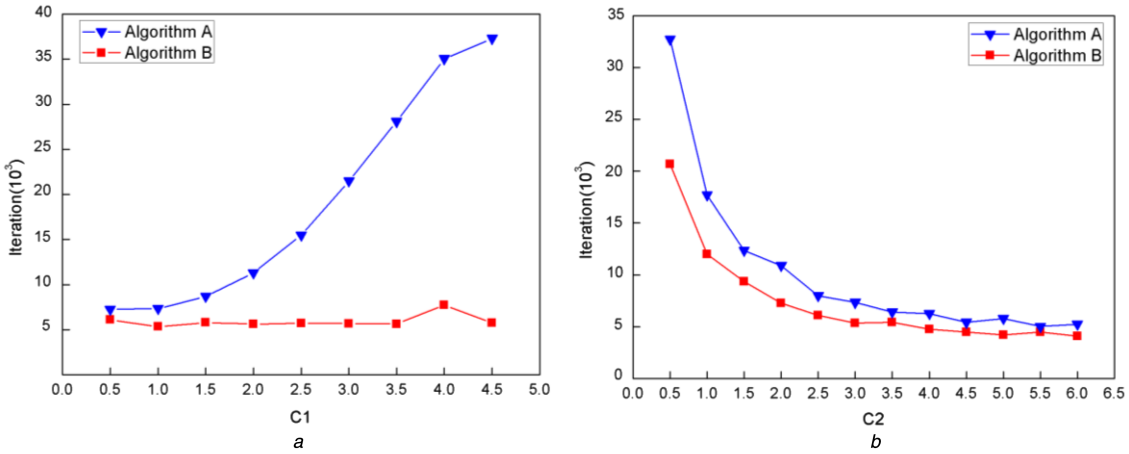

Fig. 6 *Comparison between the proposed algorithm and that pinning randomly chosen agents*
(a) Comparison of iteration number when is fixed and is changed, ***(b)*** Comparison of iteration number when is fixed and is changed

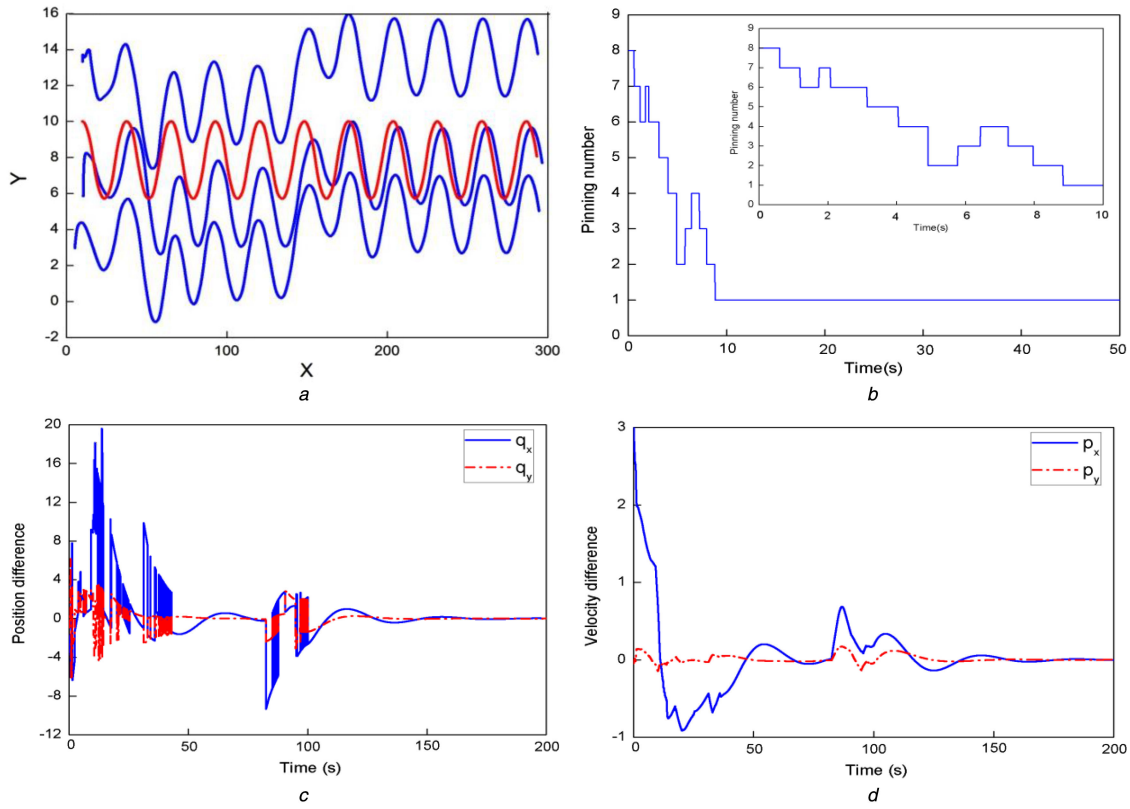

Fig. 7 *Flocking of agents following a virtual leader with varying velocity*
(a) Trajectories of three agents and the virtual leader, ***(b)*** Pinning number, ***(c)*** Position difference, ***(d)*** Velocity difference

of the informed agents from the proposed algorithm in 50 s. Figs. 7*c* and *d* show the difference of the position and velocity between the agents and the virtual leader defined as (16). These figures demonstrate that the proposed algorithm can successfully achieve the flocking behaviour for the virtual leader with a varying velocity.

6 Conclusions

A novel algorithm of dynamic pinning control for a group of agents following a virtual leader to exhibit the flocking behaviour is proposed in this work. In the DPCA, it is not assumed that the connectivity or the initial connectivity of the network. After the positions and the velocities of agents are updated, there will exist type II uninformed agents in the network. These disconnected agents are then regrouped into some connected subgroups, and then the virtual connection from the informed agent (the highest degree agent in each connected subgroup) to the virtual leader is added. In addition, we discussed the convergent rate, the number of pinning agents, and computational cost. It is shown that the proposed algorithm has a better convergent rate and less computational cost compared with those in [28]. The comparison is also made for the computational efficiency between the proposed algorithm and that pinning a randomly chosen agent. It indicates the better convergent rate and the robust stability of the proposed algorithm for the navigational feedback parameter. Furthermore, we give a modified algorithm for a group of agents to track a virtual leader with varying velocity. Numerical results show that the average positions of the informed agent and the velocities of all the agents will converge to that of the virtual leader.

7 Acknowledgments

This work was supported in part by the NSFC under grant numbers 11072086, 11372117, J1310022.

8 References

[1] Ren, W., Beard, R.W., Atkins, E.M.: 'Information consensus in multivehicle cooperative control', *IEEE Control Syst. Mag.*, 2007, **27**, (2), pp. 71–82

[2] Akyildiz, I.F., Su, W.L., Sankarasubramaniam, Y., *et al.*: 'A survey on sensor networks', *IEEE Commun. Mag.*, 2002, **40**, (8), pp. 102–114

[3] Reynolds, C.W.: 'Flocks, herds and schools: a distributed behavioral model', *Comput. Graph.*, 1987, **21**, (4), pp. 25–34

[4] Cortes, J., Martinez, S., Bullo, F.: 'Robust rendezvous for mobile autonomous agents via proximity graphs in arbitrary dimensions', *IEEE Trans. Autom. Control*, 2004, **51**, (8), pp. 1289–1298

[5] Su, H., Chen, G., Wang, X., *et al.*: 'Adaptive second-order consensus of networked mobile agents with nonlinear dynamics', *Automatica*, 2011, **47**, (2), pp. 368–375

[6] Tian, Y.P., Zhang, Y.: 'High-order consensus of heterogeneous multi-agent systems with unknown communication delays', *Automatica*, 2012, **48**, (6), pp. 1205–1212

[7] Notarstefano, G., Egerstedt, M., Haque, M.: 'Containment in leader follower networks with switching communication topologies', *Automatica*, 2011, **47**, (5), pp. 1035–1040

[8] Zhang, H.T., Zhai, C., Chen, Z.: 'A general alignment repulsion algorithm for flocking of multi-agent systems', *IEEE Trans. Autom. Control*, 2011, **56**, (2), pp. 430–435

[9] Moreau, L.: 'Stability of multi-agent systems with time-dependent communication links', *IEEE Trans. Autom. Control*, 2005, **50**, (2), pp. 169–182

[10] Ogren, P., Egerstedt, M., Hu, X.A.: 'A control Lyapunov function approach to multi agent coordination', *IEEE Trans. Robot. Autom.*, 2002, **18**, (5), pp. 847–851

[11] Hong, Y., Gao, L., Cheng, D., *et al.*: 'Lyapunov-based approach to multi-agent systems with switching jointly-connected interconnection', *IEEE Trans. Autom. Control*, 2007, **52**, (5), pp. 943–948

[12] Fax, J.A., Murray, R.M.: 'Graph Laplacians and stabilization of vehicle formations'. The 15th IFAC World Congress, Barcelona, Spain, July 2002, pp. 55–60

[13] Arcak, M.: 'Passivity as a design tool for group coordination', *IEEE Trans. Autom. Control*, 2007, **52**, (8), pp. 1380–1390

[14] Qu, Z., Wang, J., Hull, R.A.: 'Cooperative control of dynamical systems with application to autonomous vehicles', *IEEE Trans. Autom. Control*, 2008, **53**, (4), pp. 894–911

[15] Dai, J.Y., Yin, L.F., Peng, C., *et al.*: 'Research on multi-agent formation's obstacle avoidance problem based on three-dimensional vectorial artificial potential field method', *Appl. Mech. Mater.*, 2014, **596**, pp. 251–258

[16] Tanner, H.G., Jadbabaie, A., Pappas, G.J.: 'Stable flocking of mobile agents, Part I: fixed topology'. Proc. 42th IEEE Conf. on Decision and Control, Maui, December, 2003, vol. **2**, pp. 2010–2015

[17] Tanner, H.G., Jadbabaie, A., Pappas, G.J.: 'Stable flocking of mobile agents Part II: dynamic topology'. Proc. 42th IEEE Conf. on Decision and Control, Maui, December, 2003, vol. **2**, pp. 2016–2021

[18] Olfati-Saber, R.: 'Flocking for multi-agent dynamic systems: algorithms and theory', *IEEE Trans. Autom. Control*, 2006, **51**, (3), pp. 401–420

[19] Cucker, F., Smale, S.: 'Emergent behavior in flocks', *IEEE Trans. Autom. Control*, 2007, **52**, (5), pp. 852–862

[20] Yu, W.W., Chen, G.R., Cao, M.: 'Distributed leader–follower flocking control for multi-agent dynamical systems with time-varying velocities', *Syst. Control Lett.*, 2010, **59**, (9), pp. 543–552

[21] Ji, M., Egerstedt, M.B.: 'Distributed coordination control of multi-Agent systems while preserving connectedness', *IEEE Trans. Robot.*, 2007, **23**, (4), pp. 693–703

[22] Wen, G., Yu, W., Hu, G., *et al.*: 'Pinning synchronization of directed networks with switching topologies: a multiple Lyapunov functions approach', *IEEE Trans. Neural Netw. Learn. Syst.*, 2015, **26**, (12), pp. 3239–3250

[23] Wen, G., Duan, Z., Su, H., *et al.*: 'A connectivity-preserving flocking algorithm for multi-agent dynamical systems with bounded potential function', *IET Control Theory Appl.*, 2012, **6**, (6), pp. 813–821

[24] Su, H., Zhang, N., Chen, M.Z.Q.: 'Adaptive flocking with a virtual leader of multiple agents governed by locally Lipschitz nonlinearity', *Nonlinear Anal. RWA*, 2013, **14**, (1), pp. 798–806

[25] Wang, M., Su, H., Zhao, M.: 'Flocking of multiple autonomous agents with preserved network connectivity and heterogeneous nonlinear dynamics', *Neurocomputing*, 2013, **115**, pp. 169–177

[26] Wang, X.F., Chen, G.: 'Pinning control of scale-free dynamical networks', *Physica A*, 2002, **310**, (3), pp. 521–531

[27] Li, X., Wang, X., Chen, G.: 'Pinning a complex dynamical network to its equilibrium', *IEEE Trans. Circuits Syst. I*, 2004, **51**, (10), pp. 2074–2087

[28] Luo, X.Y., Liu, D., Guan, X., *et al.*: 'Flocking in target pursuit for multi-agent systems with partial informed agents', *IET Control Theory Appl.*, 2012, **6**, (4), pp. 560–569

[29] Su, H., Wang, X., Lin, Z.: 'Flocking of multi-agents with a virtual leader', *IEEE Trans. Autom. Control*, 2009, **54**, (2), pp. 293–307

[30] Hopcroft, J., Tarjan, R.: 'Efficient algorithms for graph manipulation', *Commun. ACM*, 1973, **16**, (6), pp. 372–378

[31] Khalil, H.K.: '*Nonlinear System*' (Prentice-Hall, Upper Saddle River, New Jersey, 2002, 3rd edn.)

[32] Godsil, C., Royle, G.: '*Algebraic graph theory*' (Springer-Verlag, New York, 2001)

9 Appendix

Proof of Theorem 2: Let $t_1, t_2, \ldots$ denote a series of switching time so that the switching topology $G(t)$ is the same within each of the intervals $[t_y, t_{y+1})$ for $y = 0, 1, \ldots$ Due to the switching topology, the total energy function $Q(t)$ is discontinuous at each switching time instant, but differential in each interval $[t_y, t_{y+1})$. Let $\tilde{q}_i = q_i - q_0$, $\tilde{p}_i = p_i - p_0$, $q_{ij} = q_i - q_j$ and $\tilde{q}_{ij} = \tilde{q}_i - \tilde{q}_j$. Hence the control protocol (15) for agent i is rewritten as

$$\begin{aligned} u_i = & -\sum_{j\in N_i(t)} \nabla_{\tilde{q}_i}\psi_\alpha(\|\tilde{q}_{ij}\|_\sigma) \\ & -\sum_{j\in N_i(t)} a_{ij}(q)(\tilde{p}_i - \tilde{p}_j) \\ & -h_i(t)[c_1\tilde{q}_i + c_2\tilde{p}_i] + f_0(q_0, p_0), \end{aligned} \tag{18}$$

Here, we still need the total energy function (8), and the time derivative of $Q(t)$ along the trajectories of the agents and the virtual leader is given by

$$\begin{aligned} \dot{Q}(t) = & \sum_{i=1}^{n}\sum_{j\in N_i(t)} \tilde{p}_i^{\mathrm{T}}\nabla_{\tilde{q}_i}\psi_\alpha(\|\tilde{q}_{ij}\|_\sigma) + \sum_{i=1}^{n} h_i(t)c_1\tilde{p}_i^{\mathrm{T}}\tilde{q}_i \\ & + \sum_{i=1}^{n}\tilde{p}_i^{\mathrm{T}}(u_i - f_0(q_0, p_0)) \\ = & \sum_{i=1}^{n}\sum_{j\in N_i(t)} \tilde{p}_i^{\mathrm{T}}\nabla_{\tilde{q}_i}\psi_\alpha(\|\tilde{q}_{ij}\|_\sigma) + \sum_{i=1}^{n} h_i(t)c_1\tilde{p}_i^{\mathrm{T}}\tilde{q}_i \\ & + \sum_{i=1}^{n}\tilde{p}_i^{\mathrm{T}}[-\sum_{j\in N_i(t)} \nabla_{\tilde{q}_i}\psi_\alpha(\|\tilde{q}_{ij}\|_\sigma) \\ & - \sum_{j\in N_i(t)} a_{ij}(q)(\tilde{p}_i - \tilde{p}_j) \\ & -h_i(t)(c_1\tilde{q}_i + c_2\tilde{p}_i) + f_0(q_0, p_0) - f_0(q_0, p_0)] \\ = & -\sum_{i=1}^{n}\tilde{p}_i^{\mathrm{T}}\sum_{j\in N_i(t)} a_{ij}(q)(\tilde{p}_i - \tilde{p}_j) - \sum_{i=1}^{n}\tilde{p}_i^{\mathrm{T}}h_i(t)c_2\tilde{p}_i \\ = & -\tilde{p}^{\mathrm{T}}[(L(t) + c_2H(t)) \otimes I_m]\tilde{p} \\ & \le 0 \end{aligned} \tag{19}$$

where $H(t) = \mathrm{diag}[h_1(t), h_2(t), \ldots, h_n(t)]$. In deriving (19), we have used that both $L(t)$, $H(t)$ and thus $L(t) + c_2H(t)$ are positive semi-definite matrices. The fact $\dot{Q}(t) \le 0$ implies that $Q(t)$ is a non-increasing function when $t \in [t_y, t_{y+1})$, $y = 0, 1, 2, \ldots$.

The remaining parts of the proof are the same as those in Theorem 1.